Optical Diffraction Tomography in Fluid Velocimetry: The use of A-priori Information

J Lobera and J M Coupland
Wolfson School of Mechanical and Manufacturing Engineering
Loughborough University, Ashby Road, Loughborough, Leics. LE11 3TU

Email: J.Lobera@lboro.ac.uk

Holographic Particle Image Velocimetry (HPIV) has been used successfully to make three-dimensional, three-component flow measurements from holographic recordings of seeded fluid. It is clear that measurements can only be made in regions that contain particles, but simply adding more seeding results in poor quality images that suffer from the effects of multiple scattering. Optical Diffraction Tomography provides a means to reconstruct a 3D map of refractive index from coherent recordings of scattered fields with different illumination conditions. Although the Born Approximation limits the applicability of the technique to weak-scattering problems, this approach has been used to create three-dimensional images using a Digital Holographic Microscope (DHM). A non-linear optimization technique, the Conjugated Gradient optimisation Method (CGM) has been previously proposed in microwave imaging for strong scattering problems. In this paper we propose a modification of the CGM which uses a-priori information to reduce the number of unknown variables that characterize the object to the position of the seeders. Some 2D numerical experiments have been computed, showing promising results and the value of these is fluid velocimetry is discussed.
Keywords: Holographic Particle Image Velocimetry, Digital Holography, Optical Diffraction Tomography
PACS: 42.30.Wb, 42.40.-I, 42.62.Eh

1. Introduction

Holographic Particle Image Velocimetry (HPIV) provides a means to make simultaneous three component, three-dimensional (3C3D) measurements of a seeded fluid flow[1],[2]. Implicit in the analysis of HPIV recordings is the assumption that light scattered from a laser source is recorded directly by the hologram such that multiple scattering is negligible. In practice, however, multiple scattering effects increase background noise, thereby decreasing the SNR and ultimately limiting the number of velocity vectors that can be retrieved from a given flow field[3]. The use of several recordings from different observation direction have been proposed recently[4]-[6] to mitigate this problem.

Optical Diffraction Tomography (ODT) provides a means to reconstruct a 3D map of refractive index from coherent recordings of scattered fields with different illumination conditions. It has been known for some time that if the (linear) Born approximation is assumed, the spectral (plane-wave) components of the field scattered by an object of interest are directly related spectral components that describe variation in the refractive index of the object itself[7]. Although it is noted that these measurements are incomplete, the approach has been used to create three-dimensional images of weakly scattering objects using a Digital Holographic Microscope (DHM)[8]. The assumption of weak

scattering, however, is severely restrictive as even small changes in refractive index over relatively large objects mean that multiple scattering is a dominant mechanism.

More generally we have a non-linear scattering problem and ODT, attempts to find the refractive index distribution that best explains the observed data. Recently, tomographic imaging techniques, developed for acoustic and microwave engineering, have been applied to coherent microscopy[9]. In microwave imaging, iterative methods based on the Born-Rytov approximation have been shown to improve linear inversion[10], but they still have limited applicability: to weak scattering and slow varying refractive index distributions. Newton-Kantorovich iterative methods have been developed and successfully applied in two-dimensional scalar microwave tomographic problems[11]. These methods require the inversion of large matrices, which discourage their use in three-dimensional cases. Finally, the conjugate gradient method (CGM) is an optimization technique that has been successful in microwave imaging and appears to have considerable potential in computational microscopy[12][13].

It is noted, once again, that in practice there are usually insufficient measurements to describe the refractive index distribution completely and the problem is said to be ill posed. In microwave imaging, the cost function is modified to overcome numerical instability, by introducing a regularization term that constrains the refractive index distribution. Regularization functions that have been published in the literature are mainly linear functions of the scattering potential[10],[11],[13]. Zero order, first order, second order Tikhonov stabilization operators that aim to constrain the norm, the first and the second derivative of the refractive index function respectively, have been considered. In many cases of practical interest we have steep gradients (for example walls) and large changes in refractive index and these artefacts break the conditions required by these stabilization operators.

The use of a-priori information concerning the object can simplify the problem and reduce the instabilities in the optimization. In fluid velocimetry we usually have additional information about the object, such as the diameter and the optical properties of the seeding particles. In this paper we propose a modification of the Conjugated Gradient optimization Method (CGM) that uses this information and reduces the imaging problem to that of finding the location of the particles.

In the implementation of the optimization method we need to solve the Helmholtz equation for a known refractive index distribution and illuminating field – the forward problem. Some approximations could reduce significantly the computational effort of the solver and would allow to tackle a 3D real experiment. However, this would compromise the accuracy of the forward problem and subsequently the inverse problem solution in high seeded fluids. Therefore, to show the potential of the non-linear inversion method of ODT, in this paper we use a Boundary Element Method (BEM) with a element size roughly of a tenth of the wavelength. For a typical wavelength of λ=0.633μm, this solver limits the scale of the problem that can be resolved in a desktop PC to a few microns in a 2D numerical experiment. Within this limitations, some numerical experiments have been computed that show promising results.

2. The scattering problem

According to scalar diffraction theory the (complex) amplitude of a monochromatic electric field, $E(\mathbf{r})$, propagating in a medium of (complex) refractive index, $n(\mathbf{r})$, obeys the Helmholtz equation,

$$\nabla^2 E(\mathbf{r}) + k_0^2 n^2(\mathbf{r}) E(\mathbf{r}) = 0 \tag{1}$$

where k_0 is the free space wave number defined here such that $k_0=2\pi/\lambda_0$, where λ_0 is the free space wavelength. Defining the scattering potential or object function as $\Phi(\mathbf{r}) = -k_0^2\left(n^2(\mathbf{r})-1\right)$ we can write the previous equation as

$$\left(\nabla^2 + k_0^2 - \Phi(\mathbf{r})\right) E(\mathbf{r}) = 0 \tag{2}$$

The electric field can be written as the superposition of, $E^r(\mathbf{r})$, the illuminating field (i.e. that which would be present if the object was absent) and, $E^s(\mathbf{r})$, the scattered field. Noting that $\left(\nabla^2 + k_0^2\right) E^r(\mathbf{r}) = 0$ we have,

$$\left(\nabla^2 + k_0^2\right)E^s(\mathbf{r}) = \Phi(\mathbf{r})\left(E^r(\mathbf{r}) + E^s(\mathbf{r})\right) \tag{3}$$

The terms on the right-hand-side of equation 2 can be identified as source terms and can be integrated to give

$$E^s(\mathbf{r}') = \int_{-\infty}^{+\infty} G_0(\mathbf{r}'-\mathbf{r})\Phi(\mathbf{r})\left(E^r(\mathbf{r}) + E^s(\mathbf{r})\right)d\mathbf{r}^3 \tag{4}$$

where $G_0(\mathbf{r}) = e^{jk_0|\mathbf{r}|}/|\mathbf{r}|$ is the free-space Green's Function. It is noted that a holographic microscope (or any far-field optical instrument) is only capable of measuring the propagating part of the scattered field that is observed at a distance from any inhomogeneity. In this, **r**'>> **r** and the Green's Function becomes,

$$G_0(\mathbf{r}'-\mathbf{r}) = \frac{\exp\left(j\mathbf{k}_0|\mathbf{r}'-\mathbf{r}|\right)}{|\mathbf{r}'-\mathbf{r}|} \approx \frac{e^{j\mathbf{k}_0|\mathbf{r}'|}}{|\mathbf{r}'|}\exp\left(j\mathbf{k}.\mathbf{r}\right) \tag{5}$$

where k is the wave vector defined as $\mathbf{k} = \mathbf{k}_0\mathbf{r}'/|\mathbf{r}'|$. If the measurement points are located in an sphere the curvature term will be a complex constant, and we can therefore write our observation as, $E^m(\mathbf{k})$, given by,

$$E^m(\mathbf{k}) = A\int_{-\infty}^{+\infty}\exp(-j\mathbf{k}.\mathbf{r})\Phi(\mathbf{r})\left(E^r(\mathbf{r}) + E^s(\mathbf{r})\right)d\mathbf{r}^3 \tag{6}$$

Equation 6 can be recognized as the three-dimensional Fourier Transform of the source terms of equation 3 and is general in the sense that it is based only on the assumption of scalar diffraction theory. Although $E^m(\mathbf{k})$ appears to be the full spectrum of the source terms, it is noted however, that the Fourier transform is only evaluated over a limited portion of k-space, the (Ewald) sphere, defined by $|\mathbf{k}| = 2\pi/\lambda_0$, and limited by the NA of the recording system. Consequently, the problem is generally under-determined and the scattering potential can only be estimated subject to additional properties (for example minimum variance) or certain assumptions as follows.

To evaluate the inversion method, some measurements have been computed using a Boundary Element Method (BEM) implemented as a Matlab routine to solve the forward problem. In this routine the field outside the particle is the resultant field from the scattering of a set of sources (located inside the particle). Each source scatters according to the free space Green function (in 2D, proportional to the Hankel function of the first kind). In the same way the field inside the particle is the resultant of another set of sources (located outside the particle) and scattering according to the 2D Green function in water. The appropriate weighting of these sources is obtained by enforcing the boundary condition, that reduces the problem to the inversion of a matrix. The main advantage of BEM from the Finite Element Method (FEM) is the reduction of a mesh to boundary elements and therefore the computational requirements for the matrix inversion. The field in any point can be calculated subsequently by the addition of the field scattered by the corresponding set of sources.

In the following sections, we study a 2D object of several droplets of water (n=1.33) immersed in air (n=1). To illustrate the computation of the measurements, we consider first the case of one isolated 1μm particle (figure 1a). The particle is illuminated from above and the recording system is below as in an in-line hologram. The scattered field (figure 1b) and the total field (figure 1c) has been computed in an area of 500x500 pixels that correspond to 31.6x31.6μm. The waves outside the portion of the Ewald sphere collected by a NA=0.85 have been removed (figure 1d). This filtering operation is equivalent to forward propagation to the far field recorded by a typical microscope objective and the back propagation to the position of the object, and it allows us to limit the computational task to the small area shown in the images.

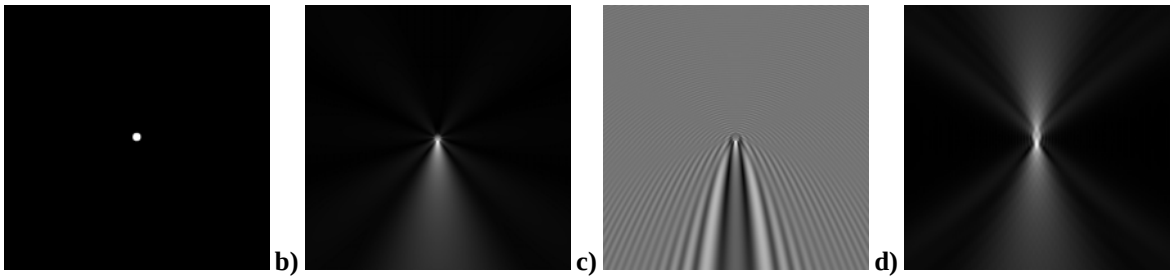

Figure 1 One 1mm-particle: a) refractive index distribution, b) absolute value of the scattered field from a vertical illumination, c) absolute value of the total field, d) measured scattered field.

A very good contrast can be appreciated in the diffraction pattern of the total field (figure 1c), therefore we can infer the scattered and incident field have roughly the same intensity. Furthermore, the phase change between the incident field and the field that goes through the particle, is roughly $\varphi \approx 2\pi d[n(r)-1]/\lambda = \pi$ for the 1μm particle. It is noted however, that although the Born approximation is not justified and the particle image is not a clear peak, it can still be located from the measurements (figure 1d).

To improve the spatial resolution in some applications, the concentration of the seed is too high to assume the scattered field is just the sum of the contributions of isolated particles. To illustrate this, in Figure 2 we show a case of 16 particles of 1μm diameter close enough so the multiple scattering between them is significant. As a consequence of the particle forward scattering, only the seed in the top of the image are illuminated by the original plane wave without distortion (figure 2c). It is noted that only these particles can be recognised from the back propagation reconstruction (figure 2d). In any case, the image we can retrieve from one measurement is confusing and inappropriate for PIV analysis. Several measurements are needed to resolve the particle location problem. In the following sections, we discuss different tomographic approaches.

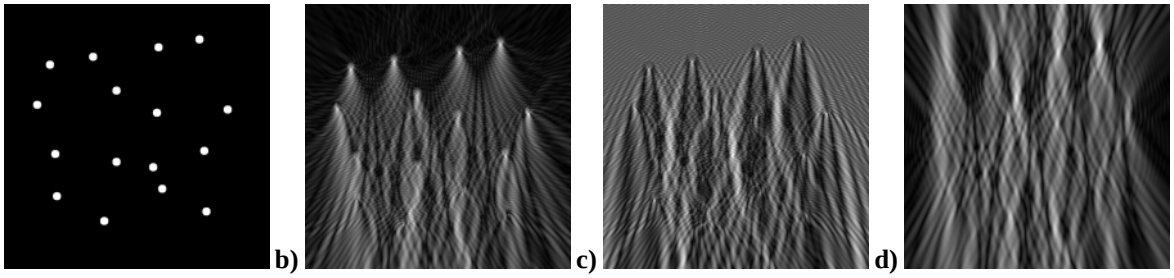

Figure 2 Sixteen particle object: a) refractive index distribution, b) absolute value of the scattered field from a vertical illumination, c) absolute value of the total field, d) measured scattered field.

3. Weak scattering approximation

Reconstruction under the assumption of weak scattering was first considered by Wolf[8] in 1969. Let us assume that we use digital holography to make a finite set of measurements E^m_{ij}, of the monochromatic plane wave components identified by the wave vectors, $\mathbf{k}_j$, that are scattered by a system which is illuminated by $E^r_i(\mathbf{r})$. Further assume that in each case the illuminating field, $E^r(\mathbf{r})$ is significantly stronger than the scattered field, $E^s(\mathbf{r})$, such that from equation 5 we have,

$$E^m_{ij} = A\int_{-\infty}^{+\infty} \exp(-j\mathbf{k}_j.\mathbf{r}) E^r_i(\mathbf{r}) \Phi(\mathbf{r})\, d\mathbf{r}^3 \tag{7}$$

An estimate of the scattering potential under the assumption of weak scattering, $\hat{\Phi}(\mathbf{r})$, can be obtained from the inverse Fourier transform of equation 7.

$$\hat{\Phi}(\mathbf{r}) = \frac{1}{A}\sum_i E^m_i(\mathbf{r}) E^r_i(\mathbf{r})^* \tag{8}$$

where $E^m_i(\mathbf{r})$ is the field computed in the whole area from the measurements at the CCD. Let us remark that according to the first Born approximation, the object function is a coherent sum of

periodic variations in refractive index that are analogous to Bragg gratings formed in a thick (volume) hologram.

For a set of measurements with a wide range of illumination and observation angles, we can cover the main part of the spectrum of the object function. To illustrate this, we have computed the measurements recorded in nine in-line holograms all around the object. The spectrum of the scattering potential obtained from these measurements (figure 2a) is sampled in every orientation, as a consequence a similar resolution can be expected in every direction. In the figure 2b) we show the absolute value of the estimated object function of one isolated particle obtained from the evaluation of the equation 8.

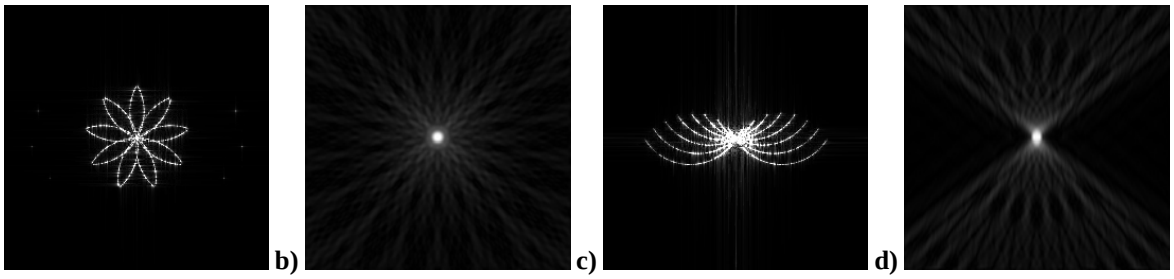

Figure 3 Born approximation for the case of full optical access in Fourier domain (a) and in spatial domain (b); and for the case of limited optical access in Fourier domain (c) and spatial domain (d).

In practice, the flow often has limited optical access. For this reason we have also computed the measurements form nine holograms with illumination angles α_i between -60 and +60 degrees and recorded with same mean observation direction (downwards). The scattering potential obtained using the Born approximation is shown in the figure 3c-d). A comparison between the figure 3a) and 3c) reveals that a different part of the object function spectrum has been reconstructed. Some higher horizontal frequencies have been included form the tilted illumination, and a better lateral resolution can be expected. But vertical frequencies have been omitted, and subsequently the impulse response is elongated in the vertical direction. In both cases, however, a clear image of the isolated particle can be obtained (compare with figure 1d).

In figure 4 we show a result when there are 16 particles in the area. In the full optical case (figure 4a), we can appreciate that the SNR of the particles located in the edges is higher than in the centre. This is due to the fact that particles at the edges have been illuminated by the plane wave without distortion for at least one of the nine recorded holograms, and correspondingly better quality image is reconstructed from this contribution (see figure 2d). For the same reason, in the limited optical access (figure 4b) only the particles towards the top of the image stand out clearly from the noise. It is noticeable that the few recognizable particles have a higher SNR than in the former case, as these particles have been benefited from the undisturbed incident field in the contributions from all the recorded holograms.

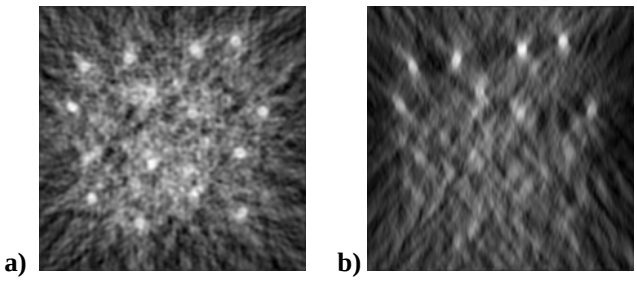

Figure 4 Born approximation object function estimation for the object recorded with a full optical access set-up (a) and with a limited optical set-up (b).

In the literature, other tomographic approaches based on the sum and on the multiplication of the reconstructed images from each hologram have been proposed[5],[6]. In order to evaluate the imaging potential of the different techniques, we compare image of similar contrast. For this purpose we have computed three magnitudes proportional to the measured field intensity (from the holograms with full optical access) according to the following equations,

$$I_{ODT}(\mathbf{r}) = \left| \sum_i E_i^m(\mathbf{r}) E_i^r(\mathbf{r}) * \right|^2 \tag{9}$$

$$I_{add}(\mathbf{r}) = \sum_i \left| E_i^m(\mathbf{r}) \right|^2$$

$$I_{mult}(\mathbf{r}) = \left[\Pi \left| E_i^m(\mathbf{r}) \right|^2 \right]^{1/N}$$

where N is the number of holograms. I_{ODT} is the square of the object function estimated with the method described previously an is shows in figure 5a. Figure 5b) and 5c) show the sum and the multiplication (to the power of 1/N) of the intensity of the different scattered fields, I_{add} and I_{mult} respectively. Let us remark that they involve similar computational effort and in all cases the effect of the multiple scattering have been neglected since they are all based in the Born approximation.

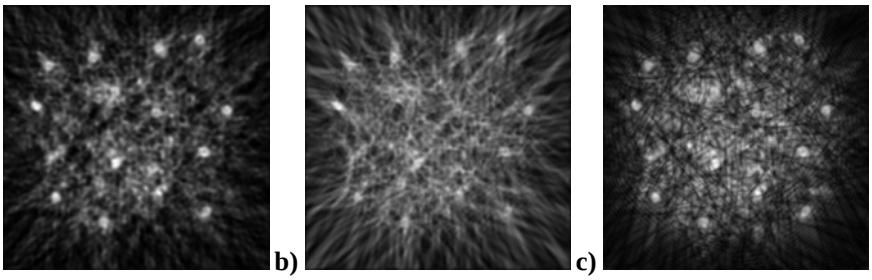

Figure 5 Comparison of three tomographic approaches: a) square of the estimated object function, b) sum of the intensity of the scattered field, c) multiplication of the intensity of the scattered field elevated to the power of 1/N.

By inspection, we can appreciate the ODT approach gives a slightly clearer image. However it is noted that the particles are not easily distinguished form the background noise.

It is clear that larger particles increases the multiple scattering and more importantly makes the scattering less similar to a point source. For a 2μm particle, the phase change between the illuminating beam and the field that goes through the particle is 2π. As a consequence the image obtained is not longer a distinct peak and appears more like a ring (figure 6a) and has two side peaks in the case of limited optical access (figure 6c).

For the same distribution of particles, the estimated object function corresponding to 2μm particles is significantly noisier (figure 6b and 6d) than for the 1μm particles (figure 4a and 4b respectively).

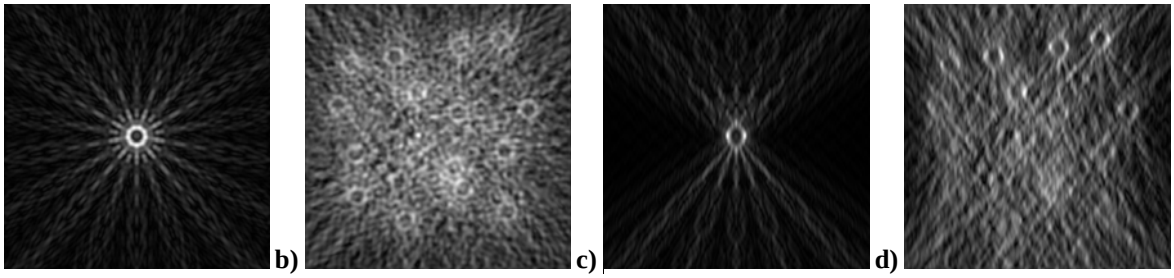

Figure 6 Estimated object function of 2μm particles: one isolated particle and sixteen particles recovered from 7 in-line holograms (a-b) and from 7 holograms recorded with a limited optical access (c-d).

The pattern of the one isolated particle shown in figure 6a (and 6c) can be seen distributed over the images in the 16 particle case of the figure 6b (and 6d respectively). This suggests that as a matched filter can be used to find a better estimation of the particle position as shown in figure 7. We can see that for every ring-shape particle image of the figure 6b it provides is a peak in the figure 7a, and similar result is obtained for the limited access case (figure 7b).

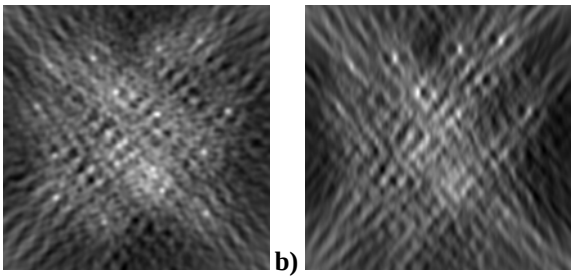

Figure 7 Matched filtered image of the sixteen 2μm-particles estimated object function for the full optical access case (a) and for the limited optical access case (b).

Let us remark, that in this way we take into account the fact that the particle does not scatter as a point source, but we continue to neglect the multiple reflections between particles. Subsequently only a few peaks stand out clearly for the background noise. To solve the inversion problem when the multiple scattering is not negligible, we need an iterative method to locate the remaining particles.

4. Optimization methods

In essence, optimization methods try to find the scattering potential that best explains the measurements of the scattered field, i.e. those which minimize the error or cost function defined by

$$J(\Phi) = \sum_{ij} \left| E_{ij}^{m} - E_{ij}^{th}(\Phi) \right|^2 \tag{10}$$

where $E_{ij}^{th}(\Phi)$ is the total field obtained by a forward solver for the illumination 'i' at the observation point 'j'. This is a non-linear optimization problem that in principle can be solved by the Conjugated Gradient Method (CGM). The search direction at the first iteration is the negative gradient of the cost function, and subsequently the component of the negative gradient that is orthogonal to the previous search direction. A line search method is used to find the strength of the increment that we need to add to the scattering potential.

For a lossless object, it can be shown[12][13] that the variation of the cost function with a differential change of the scattering potential at the **r** position, $\partial\Phi$, follows the equation

$$\frac{\partial J}{\partial \Phi} = -2 \sum_{ij} \mathrm{Re}\left((E_{ij}^{m} - E_{ij}^{th}) \frac{\partial E_{ij}^{th}\,*}{\partial \Phi} \right) \tag{11}$$

An analytical expression for $\frac{\partial E_i^{th}\,*}{\partial \Phi}$ can be obtain noticing that $E_i^{th}\,*$ should follow the equation 2 with $\Phi(r)=\Phi_\alpha(r)$ the estimated scattering potential in the previous iteration. Thus, for the iteration $\alpha+1$, the partial derivative can be written as

$$\left(\nabla^2 + k_0^2 - \Phi_\alpha(\mathbf{r}')\right) \frac{\partial E_i^{th}\,*(\mathbf{r}')}{\partial \Phi} - \delta(\mathbf{r}'-\mathbf{r}) E_i^{th}\,*(\mathbf{r}') = 0 \tag{12}$$

The integral formulation of the previous equation evaluated at the measurement points, ~~$\mathbf{r}'=$~~$\mathbf{r}_j$, gives

$$\frac{\partial E_{ij}^{th}\,*}{\partial \Phi} = \int_{-\infty}^{+\infty} G_\alpha(\mathbf{r}'-\mathbf{r}_j)\,\delta(\mathbf{r}'-\mathbf{r}) E_i^{th}\,*(\mathbf{r}')\,d\mathbf{r}'^3 = G_\alpha(\mathbf{r}-\mathbf{r}_j) E_i^{th}\,*(\mathbf{r}) \tag{13}$$

Thus, the gradient of the cost function can be expressed as

$$\partial J(\mathbf{r}) = -2 \sum_{ij} \mathrm{Re}\left(\hat{E}_i^{m}(\mathbf{r}) E_i^{th}(\mathbf{r})\,* \right) \tag{14}$$

where $\hat{E}_i^{m}(\mathbf{r}) = \sum_j G_\alpha(\mathbf{r}-\mathbf{r}_j)\left(E_i^{m}(\mathbf{r}_j) - E_i^{th}(\mathbf{r}_j)\right)$ is the back propagation of the difference between the measured and the predicted field for $\Phi_{\alpha+1}$ back propagated through the estimated object function Φ_α. For the first iteration Φ_α is zero and G_α is the free space Green function, thus the search direction of

the CGM is the real part of the scattering potential estimated with the First Born Approximation, see figure 4 for example. For the following iterations, the gradient of the cost function can also be considered as the coherent sum of Bragg holograms due to the interference between the measured minus the predicted field and the incident field, both propagated trough the object function that is computed in the previous iteration. The small features in the scattering potential, however, heavily distort the back propagated scattered field and the computed incident field through the object. As a consequence, the gradient points in the wrong direction and the optimization, after a very promising first guess, does not converge to the right solution.

To overcome the instability of the numerical implementation of the CGM, a regularization term has been used to constrain the refractive index distribution. Usually regularization terms are linear functions of the scattering potential, such as the Tikhonov stabilization operators[10],[11],[13]. However, in HPIV applications we have steep gradients in the refractive index that require edge preservation and non-linear regularization operators that are difficult to implement.

5. Use of a-priori information

As the object consists of particles of known refractive index, a reasonable assumption is that all the small features of the refractive index are noise and be can removed. Thus we propose an iterative method that estimates the location of just one particle in each iteration. From the evaluation of the gradient we can assume the most likely position to find a particle is the maximum of the gradient. However, experience has shown that the matched filtered image of the sum of the Bragg holograms, $a(\mathbf{r}) = \sum_{ij} \hat{E}_i^m(\mathbf{r}) E_i^{th}(\mathbf{r})^*$, with the estimated object function under the first Born approximation of one isolated particle gives us a clearer maximum. In this way, this iterative method estimates the location of the 1μm sixteen particles.

In the figure 8 we show the absolute value of a(**r**) in the top row, the filtered a(**r**) in the middle, and the estimated refractive index distribution with the found particles in each iteration at the bottom. The optimization has been made to stop when the error function does not decrease any further, or when the gradient intensity is below a certain threshold.

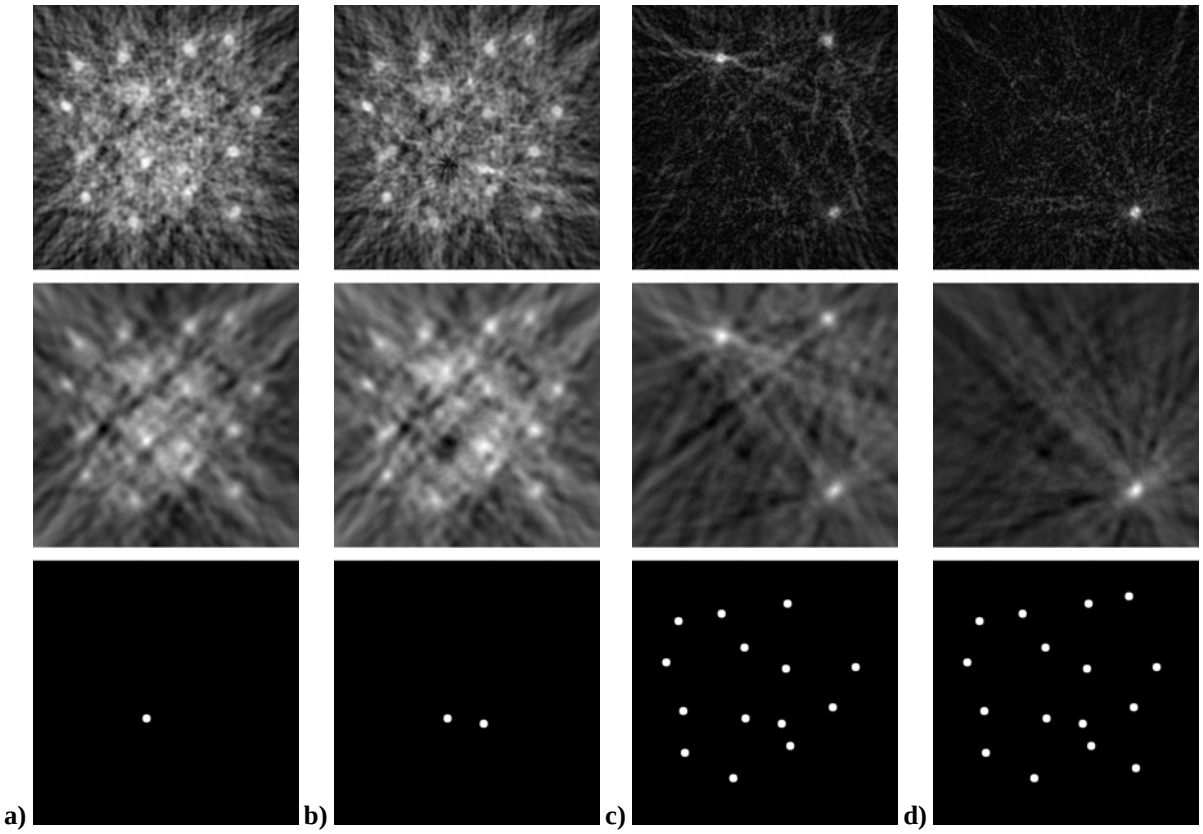

Figure 8 Optimization method in the full optical access for the 1μm particles: gradient (top), matched filtered gradient (middle) and best guess of the refractive index (bottom) for the iterations 1, 2, 14 and 16 (a, b, c and d respectively).

It is noted that after the location of the first particle, the second gradient is almost identical to the first one but one peak corresponding to the already located particle. The filtered gradient changes accordingly. In each iteration one of the peaks is removed at the same time that the others become more apparent, until the last one is found as can be seen in the right column of the figure 8.

In the case the 2μm-particles (figure 9) where the image of one particle is far from being a smooth peak, the matched filter gradient is the key to correct the location of the particle. By effectively replacing each ring-shaped particle image with a peak centered at the particle position.

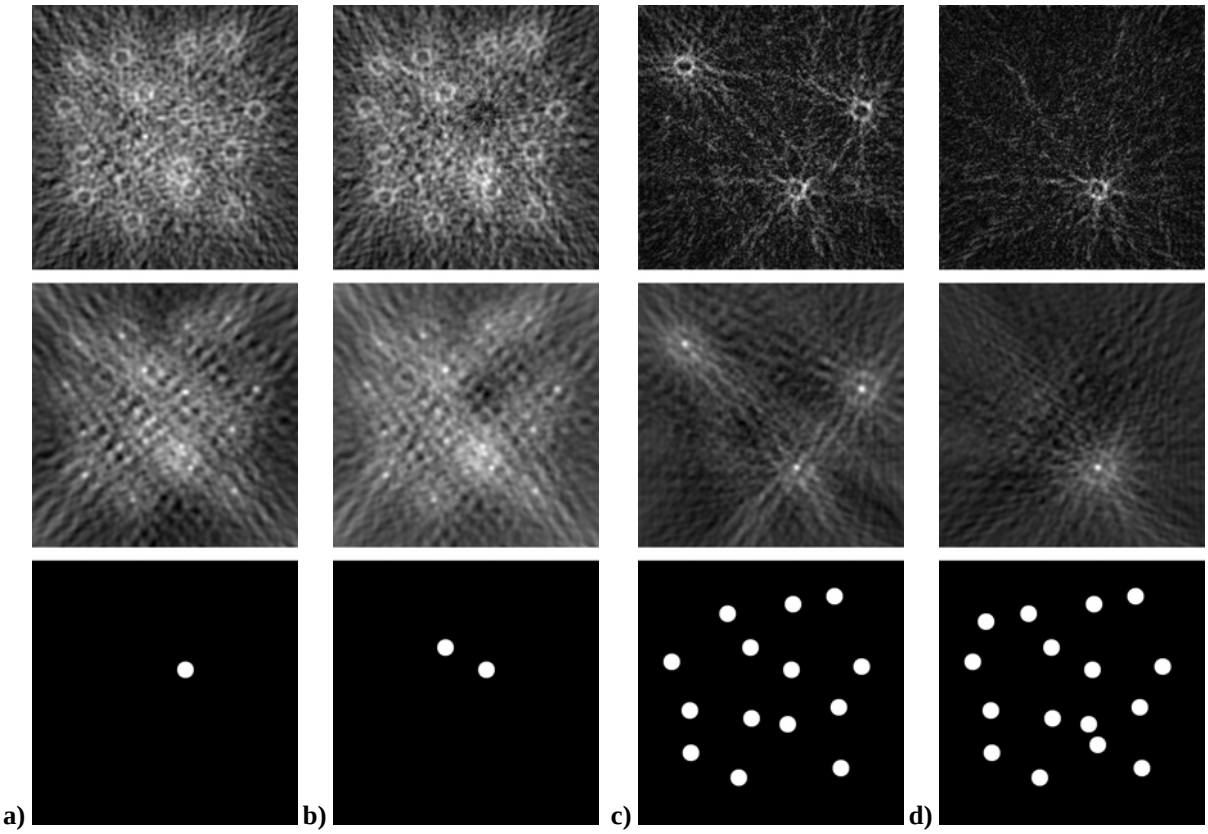

Figure 9 Optimization method the full optical access for the 2μm particles: gradient (top), matched filtered gradient (middle) and best guess of the refractive index (bottom) for the iterations 1, 2, 14 and 16 (a, b, c and d respectively).

Similar results can be obtained for the case of limited optical access as shown in figure 10 with 1μm and 2μm particles. We saw in the previous section that the different recording set-ups modify the intensity of the particle images. As a consequence the order in which the particles are located also changes.

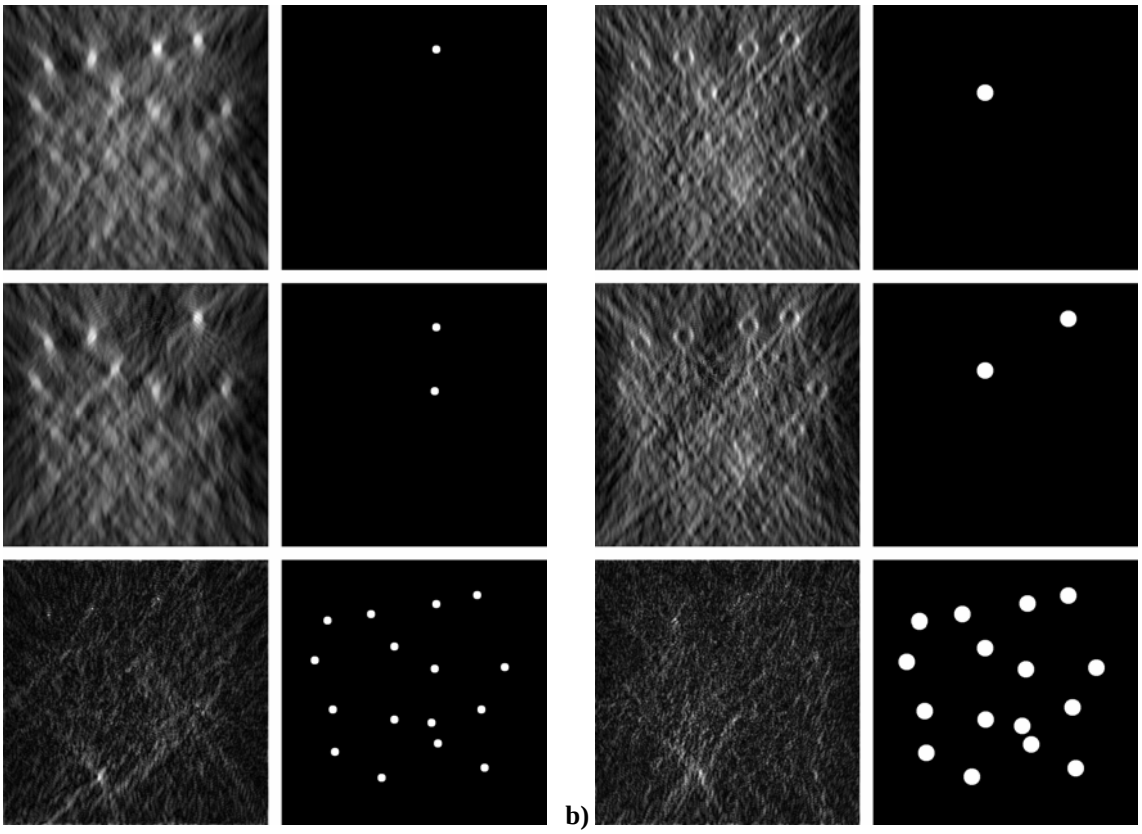

Figure 10 Gradient and refractive index distribution obtained for the first, second and sixteen iteration in the limited optical access for the 1μm particles (a) and the 2μm particles(b).

In the last iteration, the particle image obtained from the gradient of the error function is very noisy as a result of small errors in the position of the already found particles. It is clear that the identification of the first particle modifies the new computed gradient and therefore the estimated position of the other particles. In the same way, we can envisage that the located particle has affected the position of the previous peaks. As small errors can yield to a distorted gradient in the next iteration, a line search method can be used to ensure that the values for the position of the particles previously found minimize the function[14]. The computational time increases substantially and it has not being considered in the present work. The errors in the location are 0.19μm and 0.25μm for the 1μm and 2μm case respectively.

6. Conclusions

Some 2D numerical experiments have been computed to show the feasibility of the ODT techniques to identify individual particles form a set of HPIV recordings. Firstly, linear ODT has been compared with other non-linear tomographic reconstructions such as computing the sum and the multiplication of the different reconstructed intensity measured fields. It has been shown that linear ODT results in a clearer image of the particles.

When multiple scattering between particles is dominant, a non-linear inversion method is required. In this paper we have use a modification of the Conjugated Gradient Method to minimize an error function of the measured field, with the use of the a-priori information to simplify and stabilize the optimization task. We compute the gradient to obtain a first guess of the scattering potential of the object, but instead of taking it as the search direction we determine the position of one particle, and update the subsequent refractive index distribution. The maximum of the matched filtered gradient is taken as the more likely position of the particle located in each iteration.

We have shown that this method works in cases of full (360°) optical access and those in which the viewing direction is more limited.

Acknowledgments

The authors thanks the Marie Curie Action for support by the contract MEIF-CT-2005-024928.

References

[1] Coupland J.M. and Halliwell N.A. 1992 Particle image velocimetry: three-dimensional fluid velocity measurements using holographic recording and optical correlation, *Appl. Opt.* **31** 1004-8.

[2] Barnhart D.H., Adrian R.J. and Papen G.C., 1994 Phase conjugate holographic system for high resolution particle image velocimetry, *Appl. Opt.* **33**, 7159–70.

[3] Koek W.D., Bhattacharya N., Braat J.J.M., Ooms T.A. and Westerweel J., 2005, Influence of virtual images on the signal-to-noise ration in digital in-line particle holography, *Opt. Express* **13**, 2578-2589.

[4] Maas H.G., Gruen A. and Papantoniou D., 1993, Particle tracking velocimetry in three-dimensional flows. Part 1. Photogrammetric determination of particle coordinates, *Exp Fluids* **15**(2), 133-146.

[5] Sheng J., Malkiel E. and Katz J., 2003, Single beam two-views holographic particle image velocimetry, *App. Opt.* 42(2), 235-250.

Soria J. and Atkinson C., 2007, Multi-camera digital holographic imaging PIV versus Tomographic imaging PIV- Comparison and contrast of these two 3C-3D PIV techniques. *Proc. Int. Workshop on Digital Holographic Reconstruction and Optical Tomography for Engineering Applications*, Loughborough (UK). ISBN 978 0 947974 56 5, pp 27-37.

[6] Elsinga G. E., Scarano F., Wieneke B. and van Oudheusden B.W., 2005, Tomographic particle image velocimetry, *6th Int. Symp. On Particle Image Velocimetry*.

[7] Wolf E., 1969, Three-dimensional structure determination of semi-transparent objects from holographic data, *Optics Communications* **1**(4), 153-156.

[8] Lauer V., 2002, New approach to optical diffraction tomography yielding a vector equation of diffraction tomography and a novel tomographic microscope, *Journal of Microscopy* **205**(2) 165-176.

[9] Belkebir K. and Sentenac A., 2003 High-resolution optical diffraction microscopy, *J. Opt. Soc. Am. A* **20**(7), 1223-1229.

[10] Chew W.C. and Wang Y.M., 1991, Reconstruction of two-dimensional permittivity distribution using the distorted Born iterative method, *IEEE Trans. Med. Imaging* **9**, 218-225.

[11] Souvorov A.E., Bulyshev A.E., Semenov S.Y., Svenson R.H., Nazarov A.G., Sizov Y.E. and Tatsis G.P., 1998, Microwave tomography: A two-dimensional Newton iterative scheme, *IEEE Trans. Microw. Theory Tech.* **46**, 1654-1659.

[12] H., Wall D., Takenaka T. and Tanaka M., 1995, Congujated Gradient Method Applied to Inverse Scattering Problem, *IEEE Trans. Antennas Propagat.* **43**(8) 784-792.

[13] Bulyshev AE, Souvorov AE, Semenov SY, Svenson RH, Nazarov AG, Sizov YE, Tatsis GP 2000, Three-dimensional microwave tomography. Theory and computer experiments in scalar approximation, *Inverse Problems* **16**, 863-875.

[14] Lobera J. and Coupland J.M., 2007, Optical Diffraction Tomography in Digital Holographic Microscopy: Use of A-Priori Information. *Proc. Int. Workshop on Digital Holographic Reconstruction and Optical Tomography for Engineering Applications*, Loughborough (UK). ISBN 978 0 947974 56 5, pp.185-191.